Department of Computing Science,
University of Newcastle upon Tyne

ANALYSIS OF THE OSCILLATION PROBLEM IN TRI-FLOPS

O. Maevsky, D.J. Kinniment, A. Yakovlev, A. Bystrov

Technical Report Series

CS-TR-747

October, 2001

Contact:
Oleg.Maevsky@ncl.ac.uk

David.Kinniment@ncl.ac.uk

Alex.Yakovlev@ncl.ac.uk

A.Bystrov@ncl.ac.uk

Supported by EPSRC grants GR/M94366 and GR/R32666

Published by the University of Newcastle upon Tyne,
Department of Computing Science, Claremont Tower, Claremont Road,
Newcastle upon Tyne, NE1 7RU, UK

ANALYSIS OF THE OSCILLATION PROBLEM IN TRI-FLOPS

O. Maevsky, D.J. Kinniment, A. Yakovlev, A. Bystrov

29th October 2001

Abstract

A tri-flop can be used to build fast three-way arbiters. It is known that this device may exhibit oscillatory behaviour which is difficult to filter out. Using a small-signal dynamic model, this paper presents new conditions for avoiding oscillations that are more accurate than previously known. Some theoretical and practical limitations of these conditions are outlined.

1 Introduction

The metastable behaviour of a three-stable symmetric flop (tri-flop) has been investigated in [1, 2, 3]. This device can be used to build 3-way arbiters as shown in Figure 1. A metastability filter is aimed in this circuit to prevent hazards from spreading out when two or all three request signals (r1, r2, r3) arrive simultaneously.

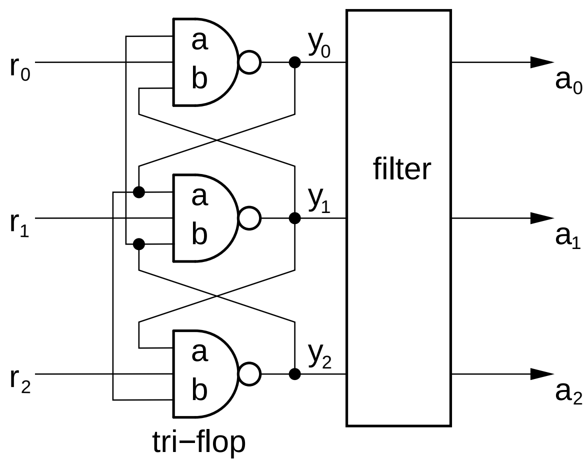

Figure 1: Three-way arbiter with a tri-flop

A detailed analysis of the tri-flop behaviour [2] shows that the metastability may actually result in oscillations on its outputs, which cannot be filtered out. The reasoning in this analysis was based on the linearised dynamic model represented as a system of ordinary linear differential equations. The solution (1) was derived in [2] as:

$$V = k_a e^{-2\frac{t}{\tau}} \begin{pmatrix} 1 \\ 1 \\ 1 \end{pmatrix} + k_b e^{\frac{t}{\tau}} \begin{pmatrix} \sin(\omega t + \varphi_0) \\ \sin\left(\omega t + \varphi_0 - \frac{2\pi}{3}\right) \\ \sin\left(\omega t + \varphi_0 + \frac{2\pi}{3}\right) \end{pmatrix}, \tag{1}$$

with

$$k_a = \frac{1}{3}(x_0 + y_0 + z_0),\ k_b = \frac{-y_0 + z_0}{\sqrt{3}\cos(\varphi_0)},$$

$$\varphi_0 = \arctan\left(\frac{2x_0 - y_0 - z_0}{\sqrt{3}(-y_0 + z_0)}\right),$$

$$\tau = \frac{2C}{G_a + G_b},\ \omega = \frac{\sqrt{3}}{2}\frac{|G_a - G_b|}{C},$$

where x_0, y_0, z_0 are initial conditions; G_a, G_b are transconductances of a and b inputs respectively (under the assumption of all gates being identical); C is a load (identical for all gates). These formulae relate the amplitude factor $e^{\frac{t}{\tau}}$and the frequency w of oscillations to the parameters G_a, G_b, and C of the model. [2] proposes to reduce the probability of hazards by minimising the difference between G_a and G_b. This reduces the frequency of oscillations and results in the slow growth of amplitude at the initial phase of metastability. It was assumed that metastability would be resolved before the amplitude grew to a significant value.

However, it is not the fact that this method eliminates the hazard completely. The linear model shows that, if there is some minimal deviation from equality between G_a and G_b, and if $|k_a| \ll |k_b|$, then the amplitudes of oscillations grow infinitely and may reach dangerously high values. The linear model has no stable states. Therefore, it makes little sense to reason about "metastable" states in such a model. The effect of saturation in a non-linear model decreases the values of transconductances G_a and G_b as the amplitude increases. The amplitude growth stops when G_a and G_b are reduced to the values where $k_b e^{1/\tau} = 1$ (when some periodic orbit is reached). Note, the amplitude factor $k_b e^{1/\tau}$ does not decrease under an attempt to minimise the frequency by making $|G_a - G_b|$ smaller (see (1)). The latter leads to a very narrow interval of initial conditions for prolonged oscillations and this complicates SPICE simulation (existing SPICE simulators have insufficient accuracy). The oscillatory metastability shown in Figure 2 is produced by the circuit in Figure 3. This circuit is implemented using "symmetrical" NAND gates from [2] with $|G_a - G_b|$. The geometry of transistors (transistor geometry is indicated in the schematic) in this example is adjusted to obtain high frequency oscillations. The realistic worst case tolerance of technological parameters may give a similar, though less vivid effect.

In this paper the linear model of the tri-flop is analysed in detail and a condition for non-oscillatory behaviour is derived. In particular, the paper shows that a more robust condition (than minimising $|G_a - G_b|$) to avoid oscillation exists, which is based on appropriate choice of CMOS technology parameters.

2 Small-signal model of gates

Let's consider the linearised model of a 2-input logical gate. The behaviour of the gate can be divided into static and dynamic parts. The static aspect is described by a Static Transfer Characteristic (STC) of a 2-input gate:

$$f(y, x_1, x_2) = 0, \tag{2}$$

where y is output and x_1, x_2 are inputs of gate.

An example of the STC shape, for a 2-NAND, is shown in Figure 4.

The dynamic aspect can be described as a motion of some point $\rho = (y, x_1, x_2)$ in the state space (within the cube of Figure 4, for example). If we take a point $\rho = (y, x_{10}, x_{20})$ outside the set of points defined by (2), then the gate will start to change its state toward the point $\rho_0 = (y_0, x_{10}, x_{20})$, such that $f(y_0, x_{10}, x_{20}) = 0$.

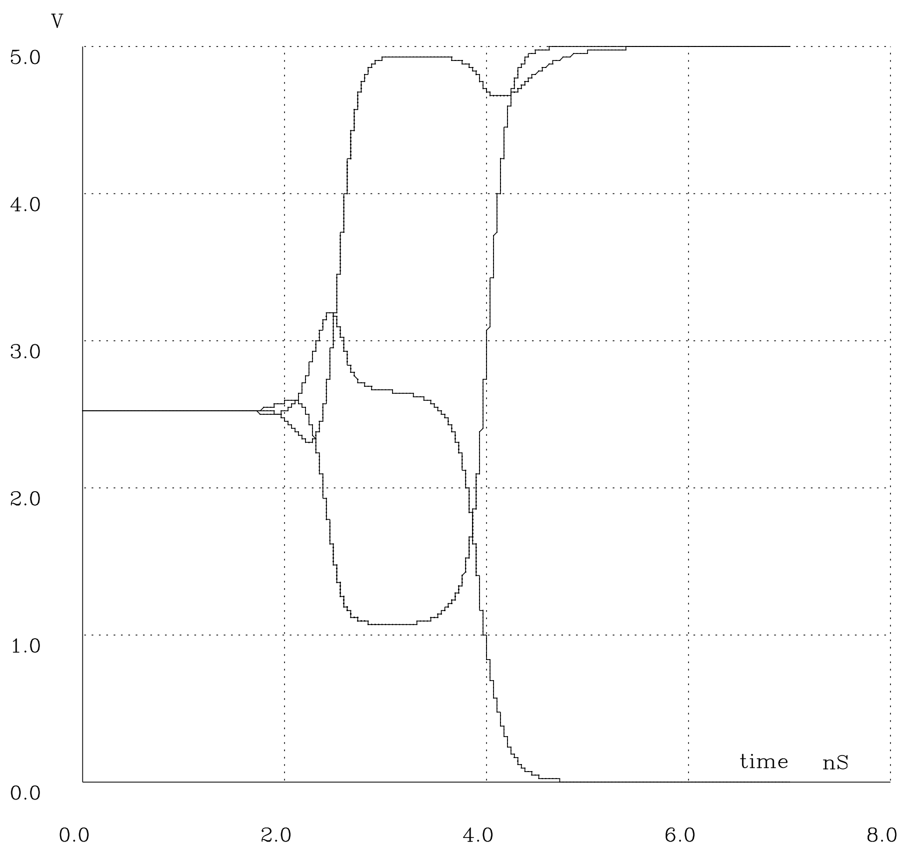

Figure 2: Oscillatory behaviour simulated in SPICE

The speed of change to y will be proportional to the magnitude of $f(y, x_{10}, x_{20})$ and directed toward surface (2). Thus, the general dynamic model of the gate can be given by the differential equation:

$$-\tau\dot{y} = f(y, x_1, x_2), \tag{3}$$

where τ is a time constant.

Equation (3) is non-linear. In the assumption that the region where oscillations may appear is small, the right part of (3) can be simplified with linear approximation. The STC has a small, almost linear, area around the point $\rho_0 = (y_0, x_{10}, x_{20})$ (see Figure 4). The linear approximation of (3) in this area allows investigating the behaviour of the gates in the most active region of its STC where an oscillatory anomalous state could take place. For linearisation it is necessary to take a Taylor series of function $f(y, x_1, x_2)$ around point $\rho_0 = (y_0, x_{10}, x_{20})$ up to its first order members.

$$\begin{aligned} f(y, x_1, x_2) \simeq\ & f(y_0, x_{10}, x_{20}) + \\ & f'_y(y_0, x_{10}, x_{20})(y - y_0) + \\ & f'_{x_1}(y_0, x_{10}, x_{20})(x_1 - x_{10}) + \\ & f'_{x_2}(y_0, x_{10}, x_{20})(x_2 - x_{20}) + ... \end{aligned} \tag{4}$$

The linearised equation of the STC follows from (4):

$$y - y_0 + S_{yx_1}(x_1 - x_{10}) + S_{yx_2}(x_2 - x_{20}) = 0, \tag{5}$$

where constants $S_{yx_1} = \frac{f'_{x_1}(y_0, x_{10}, x_{20})}{f'_y(y_0, x_{10}, x_{20})}$ and $S_{yx_2} = \frac{f'_{x_2}(y_0, x_{10}, x_{20})}{f'_y(y_0, x_{10}, x_{20})}$ are gain-factors of the gate. Thus, from (3) and (5) a linearised differential equation of a 2-input gate follows:

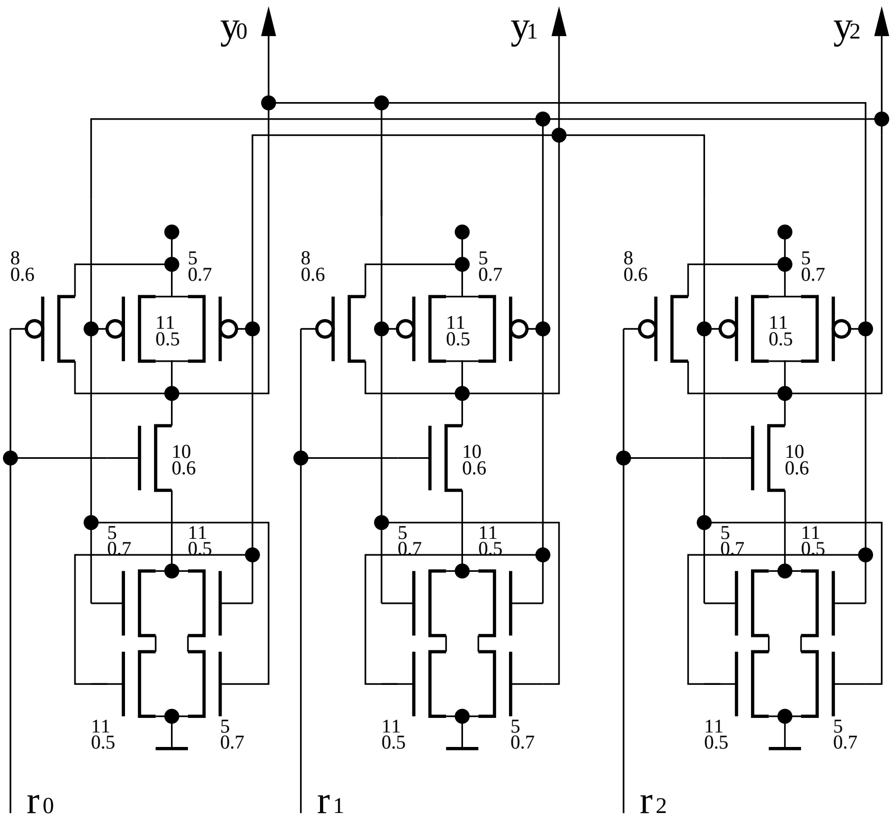

Figure 3: Transistor-level tri-flop from [2]

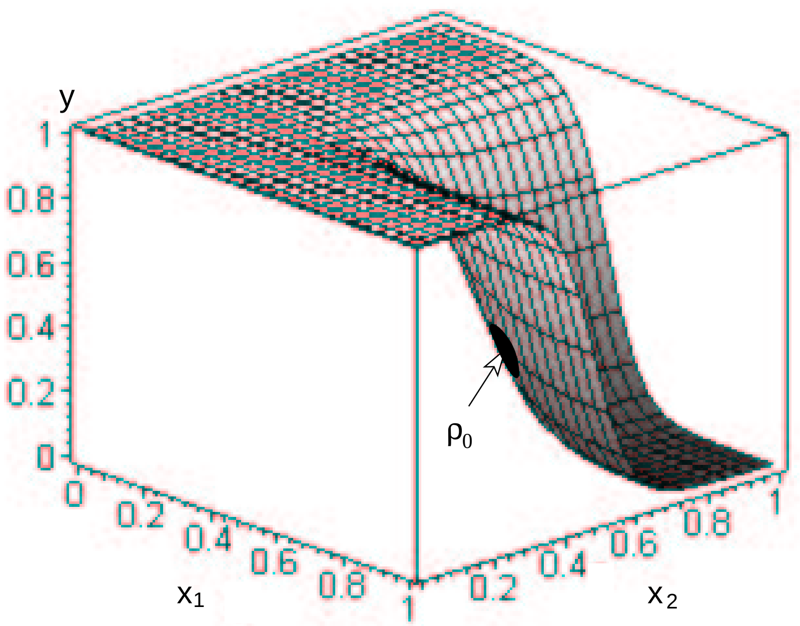

Figure 4: STC-diagram of 2-NAND

$$-\tau \dot{y} = y - y_0 + S_{yx_1}(x_1 - x_{10}) + S_{yx_2}(x_2 - x_{20}), \tag{6}$$

where $\tau = \frac{1}{f'_y(y_0,x_{10},x_{20})}$ is a time constant of a gate.

The constants S and τ can be connected with the terminology of the model of [2]. Let $\tau = \frac{1}{f'_y(y_0,x_{10},x_{20})} = \frac{C_y}{G_y}$, where C_y is the output load and G_y output conductance of the gate. This converts equation (6) to:

$$-C_y\dot{y} = G_y(y - y_0) + G_{yx_1}(x_1 - x_{10}) + G_{yx_2}(x_2 - x_{20}), \tag{7}$$

which is more accurate than the one used in [2] and corresponds to [3]. In (7), $G_{yx_1} = G_y S_{yx_1}$ is the transconductance of input x_1, and $G_{yx_2} = G_y S_{yx_2}$ is that of input x_2.

3 Small-signal model for tri-flop analysis

In the analyses of tri-flop behaviour under metastability conditions, the autonomous system shown in Figure 5 can be used.

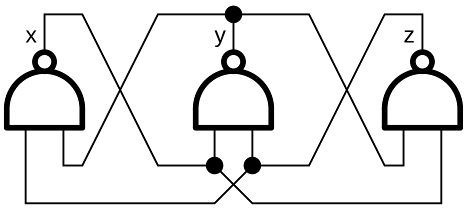

Figure 5: Autonomous model of tri-flop

According to (6), a system of three equations can be obtained:

$$\begin{cases} -\dot{x} = \frac{x-x_0}{\tau_x} + \frac{y-y_0}{\tau_{xy}} + \frac{z-z_0}{\tau_{xz}} \\ -\dot{y} = \frac{x-x_0}{\tau_{yx}} + \frac{y-y_0}{\tau_y} + \frac{z-z_0}{\tau_{yz}} \\ -\dot{z} = \frac{x-x_0}{\tau_{zx}} + \frac{y-y_0}{\tau_{zy}} + \frac{z-z_0}{\tau_z} \end{cases}, \tag{8}$$

where $1/\tau_{xy} = G_{xy}/C_x$, $1/\tau_{xz} = G_{xz}/C_x$, $1/\tau_{yx} = G_{yx}/C_y$, $1/\tau_{yz} = G_{yz}/C_y$, $1/\tau_{zx} = G_{zx}/C_z$, $1/\tau_{zy} = G_{zy}/C_z$.

It is known that oscillations around the special point $\rho_0 = (y_0, x_{10}, x_{20})$ are not possible in the non-linear model if the system (8) has no periodic solutions. The necessary condition of oscillations can be derived from the following characteristic equation:

$$p^3 + ap^2 + bp + c = 0, \tag{9}$$

where $a = \frac{1}{\tau} = \frac{1}{\tau_x} + \frac{1}{\tau_y} + \frac{1}{\tau_z}$, $b = \left(\frac{1}{\tau_x\tau_y} - \frac{1}{\tau_{xy}\tau_{yx}}\right) + \left(\frac{1}{\tau_x\tau_z} - \frac{1}{\tau_{xz}\tau_{zx}}\right) + \left(\frac{1}{\tau_y\tau_z} - \frac{1}{\tau_{yz}\tau_{zy}}\right)$, $c = \frac{1}{\tau_{xy}\tau_{yz}\tau_{zx}} + \frac{1}{\tau_{xz}\tau_{zy}\tau_{yx}} - \frac{1}{\tau_z\tau_{xy}\tau_{yx}} - \frac{1}{\tau_y\tau_{xz}\tau_{zx}} - \frac{1}{\tau_x\tau_{yz}\tau_{zy}} + \frac{1}{\tau_x\tau_y\tau_z}$.

Solutions of (8) will be not oscillatory if equation (9) has no imaginary roots. In the simple case, when $\tau_x = \tau_y = \tau_z = \tau$, the following equation can be derived from (9):

$$h^3 + Ah + B = 0, \tag{10}$$

where $h = p + 1/\tau$, $A = -\frac{1}{\tau_{xy}\tau_{yx}} - \frac{1}{\tau_{xz}\tau_{zx}} - \frac{1}{\tau_{yz}\tau_{zy}}$, $B = \frac{1}{\tau_{xy}\tau_{yz}\tau_{zx}} + \frac{1}{\tau_{xz}\tau_{zy}\tau_{yx}}$.

Equation (10) has no imaginary roots if the following inequality holds:

$$Q = \frac{B^2}{2^2} + \frac{A^3}{3^3} \le 0. \tag{11}$$

So, assuming that $\tau_{xy} = \tau_{yx} = 1/\varepsilon_1$, $\tau_{xz} = \tau_{zx} = 1/\varepsilon_2$, $\tau_{yz} = \tau_{zy} = 1/\varepsilon_3$ inequality (11) is reduced to a classical one:

$$\sqrt[3]{\varepsilon_1\varepsilon_2\varepsilon_3} \leq \frac{\varepsilon_1^2 + \varepsilon_2^2 + \varepsilon_3^2}{3}, \tag{12}$$

which is always true. Under another assumption, such as $\tau_{xy} = \tau_{xz} = 1/\varepsilon_x$, $\tau_{yx} = \tau_{yz} = 1/\varepsilon_y$, $\tau_{zx} = \tau_{zy} = 1/\varepsilon_z$, the following can be obtained by the analogy to inequality (12).

$$\sqrt[3]{\frac{1}{\varepsilon_x\varepsilon_y\varepsilon_z}} \leq \frac{\frac{1}{\varepsilon_x} + \frac{1}{\varepsilon_y} + \frac{1}{\varepsilon_z}}{3} \tag{13}$$

Thus, oscillations can be avoided even when the difference between G_a and G_b is of considerable value, contrary to the recommendation in [1]. Equality $G_a = G_b$ allows only reaching the minimal satisfaction of condition (11), presenting a very little safety margin in terms of technology parameter variations. However, it clearly follows from (12) and (13) that inequality (11) can be satisfied more strongly by suitable choice of a proportion between the gains of the gates. Figure 6 shows Q as a function (11) of a deviation parameter d, where $1/\tau = 10$, $\tau_{xz} = \tau$, $1/\tau_{xy} = 1/\tau - d/\tau$, $1/\tau_{yx} = 1/\tau - d/\tau$, $1/\tau_{yz} = 1/\tau + d/\tau$, $1/\tau_{zy} = 1/\tau + d/\tau$, $\tau_{zx} = \tau$.

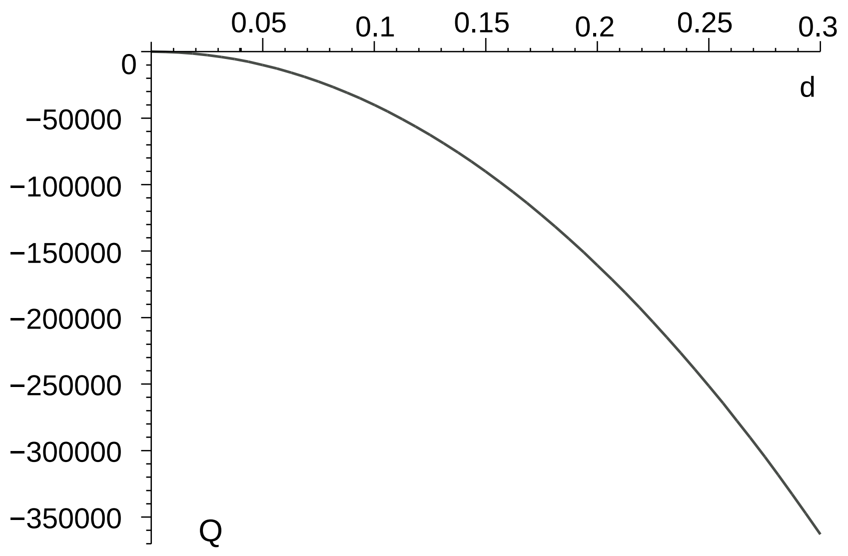

Figure 6: Conditions of imaginary roots absence

Thus, if to take $1/\tau = 10$ and $d = 0.1$, then $1/\tau_{xz} = 10$, $1/\tau_{xy} = 9$, $1/\tau_{yx} = 9$, $1/\tau_{yz} = 11$, $1/\tau_{zy} = 11$, $1/\tau_{zx} = 10$, and $Q \simeq -40000$. The 10% deviation of $1/\tau$ can easily be arranged by suitable transistor sizes.

For comparison, in the opposite situation, when $1/\tau = 10$, and $1/\tau_{xz} = 1/\tau + d/\tau$, $1/\tau_{xy} = 1/\tau - d/\tau$, $1/\tau_{yx} = 1/\tau + d/\tau$, $1/\tau_{yz} = 1/\tau - d/\tau$, $1/\tau_{zy} = 1/\tau + d/\tau$, $1/\tau_{zx} = 1/\tau - d/\tau$, the worst case takes place, and the existence of imaginary roots is satisfied, as shown in Figure 7 similar to the example in Figure 3.

In the general case, when $\tau_x \neq \tau_y \neq \tau_z$, the condition of imaginary roots absence matches (11):

$$Q = \frac{q^2}{2^2} + \frac{p^3}{3^3} \leq 0, \tag{14}$$

where $q = \frac{a}{3}\left(2\frac{a^2}{9} - b\right) + c$; $p = -\frac{a^2}{3} + b$.

Expanding these formulae:

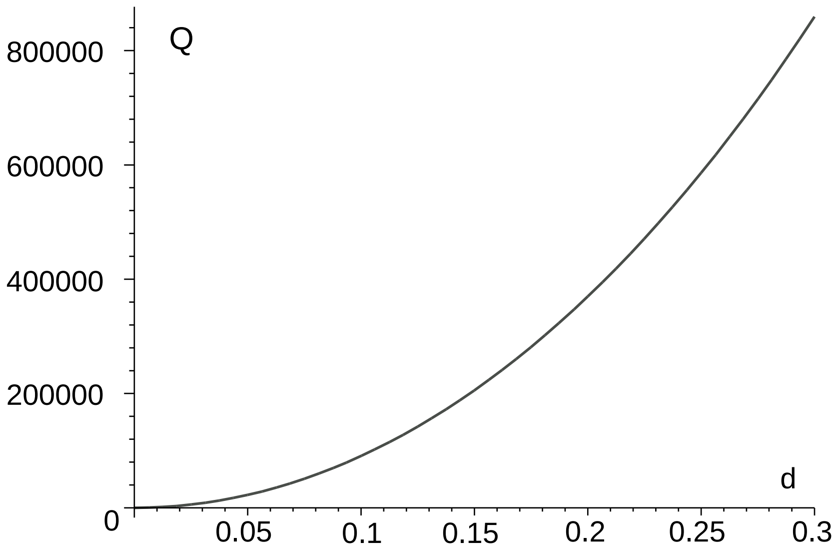

Figure 7: Conditions of imaginary roots existence

$$\begin{aligned} q \;=\;& \frac{2aL}{27} + \\ & \frac{1}{9}\left[\left(\frac{1}{\tau_x}+\frac{1}{\tau_y}\right)\left(\frac{3}{\tau_{xy}\tau_{yx}}-\frac{1}{\tau_x\tau_y}\right)+\right. \\ & \left(\frac{1}{\tau_x}+\frac{1}{\tau_z}\right)\left(\frac{3}{\tau_{xz}\tau_{zx}}-\frac{1}{\tau_x\tau_z}\right)+ \\ & \left.\left(\frac{1}{\tau_y}+\frac{1}{\tau_z}\right)\left(\frac{3}{\tau_{yz}\tau_{zy}}-\frac{1}{\tau_y\tau_z}\right)\right]- \\ & \frac{2}{3}\left(\frac{1}{\tau_{xy}\tau_{yx}\tau_z}+\frac{1}{\tau_{xz}\tau_{zx}\tau_y}+\right. \\ & \left.\frac{1}{\tau_{yz}\tau_{zy}\tau_x}-\frac{1}{\tau_x\tau_y\tau_z}\right)+B \end{aligned} \tag{15}$$

and

$$p = -\frac{L}{6} - A, \tag{16}$$

where $L = \left(\frac{1}{\tau_x}-\frac{1}{\tau_y}\right)^2 + \left(\frac{1}{\tau_x}-\frac{1}{\tau_z}\right)^2 + \left(\frac{1}{\tau_y}-\frac{1}{\tau_z}\right)^2$.
Then with (15), (16) and with the assumption that (11) is true, inequality (14) can be reduced to

$$\begin{aligned} (\tau_z-3\tau)\,(3S_{xy}S_{yx}-1) \quad &+ \\ (\tau_y-3\tau)\,(3S_{xz}S_{zx}-1) \quad &+ \\ (\tau_x-3\tau)\,(3S_{yz}S_{zy}-1) \quad &\leq \quad -\tfrac{2}{3}L \end{aligned} \tag{17}$$

The inequality (17) determines the area where equation (9) has no imaginary roots. As a result of (17), for example, the solutions of (8) will not be oscillatory if the following system, with strict satisfaction of the order of subscripts, is true (with (12) or (8)):

$$\begin{cases} S_{yz}S_{zy} \geq S_{xz}S_{zx} \geq S_{xy}S_{yx} \\ \tau_z \geq \tau_y \geq \tau_x \end{cases} \tag{18}$$

Unfortunately, the last condition is not formally equivalent to (17). It can, however, be used as a good practical heuristic in the search for a solution to (17). A solution is sought by keeping the differences between products SS greater than those between τ's.

4 Conclusions

This paper has presented new conditions for oscillatory behaviour of a tri-flop, the key element of a three-way arbiter. These conditions are more refined compared to those of [2]. They are based on a more accurate dynamic model of a gate, corresponding to [3].

One should however realise two fundamental aspects that may be on the way of immediate use of the derived conditions.

The first aspect is theoretical. The conditions of the absence of oscillations have to be true for all of the special points in the phase space of the nonlinear system (19) of a tri-flop:

$$\begin{cases} -\tau_x \dot{x} = f_x(x,y,z) \\ -\tau_y \dot{y} = f_y(y,x,z) \\ -\tau_z \dot{z} = f_z(z,y,x) \end{cases} \tag{19}$$

There are four such points, where system (19) can be in unstable equilibrium (metastability points); they are the solutions of the following system:

$$\begin{cases} f_x(x,y,z) = 0 \\ f_y(y,x,z) = 0 \\ f_z(z,y,x) = 0 \end{cases} \tag{20}$$

These points correspond to those considered in [2]. Correct investigation of the system requires considering linear approximations of the system around each of the metastable points separately. These points are usually so remote from each other that non-linearity cannot be avoided.

The second aspect is more practical. All the parameters of linear dynamic model (τ, G, S) are related to the parameters of the physical model in a very complex manner. For example, modelling a gate (say, z) as a simple resistor-based circuit (in small-signal domain) leads to the function:

$$z = \frac{E\left(\frac{1}{R_{px}(x)} + \frac{1}{R_{py}(y)}\right)(R_{nx}(x) + R_{ny}(y))}{1 + \left(\frac{1}{R_{px}(x)} + \frac{1}{R_{py}(y)}\right)(R_{nx}(x) + R_{ny}(y))}. \tag{21}$$

where $R_{px}(x)$, $R_{py}(y)$, $R_{nx}(x)$, $R_{ny}(y)$ are the resistances of the n- and p-types transistors when the system is in the metastable state. Such a function should be obtained by taking the Taylor series in the each metastable point of the system (19), as it was done above. Functions $R_{px}(x)$, $R_{py}(y)$, $R_{nx}(x)$, $R_{ny}(y)$ create correlation of parameters between linear and physical models. According to [4], function $R_{nx}(x)$, for example, has the form: $R_{nx}(x) = \frac{2E}{\beta_n(E-e_n-x)}$, where E is a supply voltage, e_n threshold voltage of n-type transistor, $\beta_n = MUZ \cdot C'_{ox} \cdot \frac{W_{nx}}{L_{nx}}$, and MUZ zero-bulk-bias mobility, C'_{ox} oxide capacitance, $\frac{W_{nx}}{L_{nx}}$ the width to length ratio of a x-transistor channel. Thus it is clear, that the transistor gain β, the most important parameter, is non-linear and in complex correlation with the dynamic model gain S. Because of these complexities it is difficult to give universal recommendations to build reliable arbiters on a tri-flop basis, but transistor width variations in the rations suggested here should provide a good enough safeguard. To refine a technique of tri-flop arbiter development to a perfection it is necessary to carry out further investigations.

References

[1] D.J. Kinniment, A. Yakovlev and B. Gao, "Metastable behaviour and system performance," Proc. of 2nd UK Forum on Asynchronous Systems, Newcastle upon Tyne, July 1997.

[2] C.H. van Berkel and C.E. Molnar,"Beware the 3-Way Arbiter," IEEE Journal of Solid-State Circuits, Vol.34, pp. 840-848, 1999.

[3] A.C. Davies,"Dynamic Properties of a Multiway Arbiter," ISCAS 2000 - IEEE International Symposium on Circuits and Systems, May 28-31, 2000, Geneva, Switzerland, pp. III-221-224.

[4] R.J. Baker, H.W. Li, and D.E. Boyce, "CMOS Circuit Design, Layout, and Simulation," Institute of Electrical and Electronics Engineers, New York, 1998.